Journal of Computational Physics **176,** 345–362 (2002)
doi:10.1006/jcph.2002.6991, available online at http://www.idealibrary.com on IDEAL®

A Stable Scheme for the Numerical Computation of Long Wave Propagation in Temporal Laminates

Suzanne L. Weekes

Department of Mathematical Sciences, Worcester Polytechnic University, Worcester, Massachusetts 01609-2280
E-mail: sweekes@wpi.edu

Received March 26, 2001; revised December 7, 2001

A temporal laminate is a material whose parameters are homogeneous in space but vary periodically and discontinuously in time. In this article, we consider wave propagation through a temporal laminate where the period of the disturbance moving through the media is large relative to ε the period of the lamination. It is worth noting that the constituent materials and the mixing coefficient can be chosen so that the effective speed in a temporal laminate is *greater* than the individual phase speeds. We show that the analytic problem admits stable long wave modes, but shorter wave modes grow as they pass through the laminate layers. Computing wave motion through this composite medium using the standard upwind, finite-difference method under the CFL condition for numerical wave propagation in the individual media will produce growing short wave modes. Numerical results are degraded since accuracy is quickly lost due to the growth of short waves which enter into the computation through truncation and round-off error. A new CFL constraint is derived for a finite-difference numerical scheme which will allow us to compute the stable long wave motion. Numerical results are given for the direct numerical simulation of the homogenization problem ($\varepsilon \to 0$).

Key Words: stability; composite materials; finite difference; CFL; discontinuous coefficients; wave propagation; dynamic materials.

1. INTRODUCTION

In this paper, we consider wave propagation through a one-dimensional temporally laminated medium. A temporal laminate is a material whose parameters are homogeneous in space but vary periodically and discontinuously in time. As an example of such, consider an electric transmission line where the inductance and capacitance fluctuate between two states. The change in capacitance can be effected by the use of piezoelectric materials,

0021-9991/02 $35.00

while the inductance variation may be accomplished by varying the permeability in the ferromagnetic material in which the line is embedded.

The governing equation for wave motion through a temporal laminate is

$$(\rho z_t)_t - k z_{xx} = 0.$$

The parameters $\rho(t)$ and $k(t)$ may be the density and stiffness of a slender elastic rod subject to longitudinal disturbances z, or the dielectric permittivity and the reciprocal of magnetic permeability of a medium through which a plane electromagnetic wave with electric field component $E = z_t$ propagates. For a temporal laminate, we make the following specific assumptions about the composite medium:

(a) at each point (x, t), the controls ρ and k can take either the values (ρ_1, k_1) or (ρ_2, k_2); we refer to these as "material 1" and "material 2";

(b) the period of the pattern is composed of two successive layers filled, respectively, by materials 1 and 2, the volume fractions of these layers being m_1 and m_2 ($m_1, m_2 \geq 0, m_1 + m_2 = 1$);

(c) these materials are placed within alternating layers $t = \text{const}$.

On the interfaces $t = n\varepsilon$ and $t = (n + m_1)\varepsilon$ for $n = 0, 1, 2, \ldots$, we require a regular transition of continuous disturbance $z(x, t)$, and enforce kinematic and dynamic compatibility conditions across the material interfaces.

Temporal laminates are a special subgroup of the class of composites that we call dynamic materials. Dynamic materials are formations assembled from materials distributed on a microscale in time and in space. Optimal material design for static or nonsmart applications generally results in the formation of composites where the design variables, such as material density, stiffness, yield force, and other structural parameters are position dependent, but invariant in time. The structures that result from these designs are the ordinary composite materials, and their properties depend on the individual properties of the constituent materials and the microgeometry of the mixture. The effective property of a dynamic material, however, also depends on the temporal arrangement, so by varying the spatio-temporal parameters in the material mixture, we can effect a range of responses some of which are unachievable through purely spatial material design [1–3].

A temporal laminate is one of the limiting cases of a *spatio-temporal laminate*. Spatio-temporal laminates are defined by (a)–(b) with (c) replaced by the condition that the materials are placed within alternating layers having the slope $dx/dt = V$ on the (x, t)-plane. In a temporal laminate, $V = \infty$. The other limiting case when $V = 0$ gives the ordinary static laminate. Static laminates have been well studied analytically ([4–9]), and have been studied computationally in [10] and [3], for example. The numerical study by this author in [3] is of the class of subsonic spatio-temporal laminates where $|V| < a_1, a_2$ for $a_i = \sqrt{k_i/\rho_i}$, the characteristic speed in material i. The current study of wave motion in temporal laminates is a step towards successfully computing wave motion in supersonic laminates ($|V| > a_i$.)

It has been illustrated analytically and numerically [1–3] that the performance of structures can be improved by using spatio-temporal composites which match the time dependent environment of dynamic problems. By appropriately controlling the design factors of a dynamic laminate, it is possible to selectively screen large domains in space–time from the invasion of long wave disturbances, which may take the form of surges of stress waves and other undesirable impulses in the structure or mechanism. With an ordinary static composite,

this *screening effect* is impossible. This screening effect is responsible for the appearance of such important phenomena as the elimination of the cutoff frequency in appropriately activated electromagnetic wave guides. In addition, it is responsible for the appearance of "left-handed" composite materials—materials which have been *theorized*, and only recently physically *realized*, to reverse some known physical effects observed in ordinary materials in response to electromagnetic radiation, such as the Doppler frequency shift and Cherenkov radiation (see News Release NSF PR00-9).

In [1], a standard analytical homogenization procedure is used to calculate the effective phase velocities and the governing differential equations in a spatio-temporal composite when the period of the medium, ε, is much smaller than the wavelength of the initial disturbance. Using the notation $\langle\xi\rangle = m_1\xi_1 + m_2\xi_2$ and $\bar{\xi} = m_1\xi_2 + m_2\xi_1$, it is found that $\langle z\rangle$, the value of the disturbance z averaged over the period of the array, obeys the following differential equation:

$$\frac{1}{a_1^2 a_2^2}\left[V^2 - \bar{k}\left(\frac{\bar{1}}{\rho}\right)\right]\langle z\rangle_{tt} + 2V\left[\bar{\rho}\left(\frac{\bar{1}}{k}\right) - \left(\frac{\bar{1}}{a^2}\right)\right]\langle z\rangle_{tx} - \bar{\rho}\left(\frac{\bar{1}}{k}\right)\left[V^2 - \frac{1}{\bar{\rho}\left(\frac{\bar{1}}{k}\right)}\right]\langle z\rangle_{xx} = 0.$$

It is then straightforward to deduce that in temporal laminates ($V = \infty$), the effective governing equation is

$$\langle z\rangle_{tt} - \langle 1/\rho\rangle\langle k\rangle\langle z\rangle_{xx} = 0, \tag{1}$$

and the effective wave velocities are

$$\pm\sqrt{\langle 1/\rho\rangle\langle k\rangle}. \tag{2}$$

We note that one can choose parameters ρ_i, k_i such that the effective speed in the temporal laminate is *greater* than the individual phase speeds in the constituent materials.

It is helpful to recast the second-order scalar problem as a first-order system in z and a dual variable v:

$$z_t - \frac{1}{\rho}v_x = 0, \tag{3}$$

$$v_t - kz_x = 0. \tag{4}$$

In this formulation, the interface condition is that z and v remain continuous through the transition; thus we are looking at a sequence of a pair of initial value problems. Letting $n = 0, 1, 2, \ldots$ index the sequence, the IVP pair consists of the PDE system above for $t \in [n\varepsilon, (n + m_1)\varepsilon]$ with $(k, \rho) = (k_1, \rho_1)$ and data given at $t = n\varepsilon$, followed by the system with parameters (k_2, ρ_2) for $t \in [(n + m_1)\varepsilon, (n + 1)\varepsilon]$, and initial data given at $t = (n + m_1)\varepsilon$.

In the exact solution to the analytic problem, the shorter wave components are amplified as they go from one material layer to the next, though they do not grow within a region of pure material. As the laminate period ε gets smaller, or as time gets larger these modes will grow without bound. There is an *inherent instability* to the problem. However, we are interested only in studying long wave motion through the medium. By "long," we mean disturbances consisting of modes with wave number ω such that $\varepsilon\omega$ is small enough that these modes remain bounded in time. Our goal is to find a scheme that reproduces the stable long wave motion in the limit $\varepsilon \to 0$.

This article proceeds as follows. In the next section, we prove that a general disturbance imparted to a temporal laminate will exhibit inherent instability, with some wave modes growing and longer wave modes remaining stable. In Section 3, we show that even under the accepted CFL condition, which ensures stability for the wave problem in the individual materials, the first-order finite difference approximation to the temporal lamination problem may give unstable results. Long wave initial disturbances which are stable analytically can be degraded in the computation due to the introduction of shorter wave modes coming from round-off and truncation errors. We derive stability conditions for a computational scheme which will damp out the shorter wave modes and thus retain the integrity of the numerical results. In the final section, we conclude by giving a numerical example to support our results.

2. INHERENT INSTABILITY OF THE ANALYTIC PROBLEM

The system of equations (3) and (4) can be decoupled into two advection equations in the characteristic variables $z - v/\mu$ and $z - v/\mu$:

$$\begin{pmatrix} z + v/\mu \\ z - v/\mu \end{pmatrix}_t + \begin{pmatrix} -a & 0 \\ 0 & a \end{pmatrix} \begin{pmatrix} z + v/\mu \\ z - v/\mu \end{pmatrix}_x = \begin{pmatrix} 0 \\ 0 \end{pmatrix}. \tag{5}$$

We use μ to denote the material "impedances" $\sqrt{k\rho}$. It is easily seen now that information $z - v/\mu$ and $z + v/\mu$ travel along characteristic lines with respective characteristic velocities $\pm a$, where $a = \sqrt{k/\rho}$, so that $(z - v/\mu)(x, t) = (z - v/\mu)(x - at, 0)$ and $(z + v/\mu)(x, t) = (z + v/\mu)(x + at, 0)$. At any point in space–time $z(x, t) = \frac{1}{2}[(z + v/\mu) + (z - v/\mu)](x, t)$ and $v(x, t) = \frac{\mu}{2}[(z + v/\mu) - (z - v/\mu)]$.

The wave equation with ρ and k constant is stable. An initial impulse consisting of a single wave mode of wavenumber ω, $(z, v)(x, t) = (\bar{z}, \bar{v})e^{i\omega x}$ at time t evolves according to the growth or amplification matrix G so that $(z, v)(x, t + \Delta t) = G(\omega, \Delta t)(z, v)(x, t) = Q^{-1}S(\omega, \Delta t)Q$. Here Q is the transformation from the primary variables z and v to the characteristic variables $z + v/\mu$ and $z - v/\mu$, and S is the growth matrix of the characteristic variables,

$$Q = \begin{pmatrix} 1 & 1/\mu \\ 1 & -1/\mu \end{pmatrix}, \quad S = \begin{pmatrix} e^{i\omega a \Delta t} & 0 \\ 0 & e^{-i\omega a \Delta t} \end{pmatrix},$$

since $(z - v/\mu)(x, t) = (z - v/\mu)(x - at, 0)$ and $(z + v/\mu)(x, t) = (z + v/\mu)(x + at, 0)$. Thus,

$$G = \begin{pmatrix} \frac{1}{2}(e^{i\omega a \Delta t} + e^{-i\omega a \Delta t}) & \frac{1}{2\mu}(e^{i\omega a \Delta t} - e^{i\omega a \Delta t}) \\ \frac{\mu}{2}(e^{i\omega a \Delta t} - e^{i\omega a \Delta t}) & \frac{1}{2}(e^{i\omega a \Delta t} + e^{i\omega a \Delta t}) \end{pmatrix} = \begin{pmatrix} \cos(\omega a \Delta t) & i\frac{1}{\mu}\sin(\omega a \Delta t) \\ i\mu \sin(\omega a \Delta t) & \cos(\omega a \Delta t) \end{pmatrix}.$$

We note that $G(\omega, \Delta t) = G(\omega a \Delta t)$. The eigenvalues of G (and S) are clearly $e^{\pm i\omega a \Delta t}$, thus the norm of the eigenvalues is 1, regardless of a, Δt, or ω. There are no growing modes and the constant coefficient problem is unconditionally stable.

For the laminate problem, we consider mode growth of a wave pulse traveling through a layer of material 1 for time $\Delta t_1 = m_1\varepsilon$ and then a layer of material 2 for a time $\Delta t_2 = m_2\varepsilon$. The interface condition is that z and v remain continuous throughout the transition; thus we

are looking at a sequence of initial value problems. The initial data for the problem at the interface of material 1 and 2 are thus $G_1(\omega a_1 \Delta t_1)(\bar{z}, \bar{v})e^{i\omega x}$, so the growth of a disturbance with wavenumber ω is governed by the matrix

$$
\begin{aligned}
G_{1,2}(\omega, \Delta t_1, \Delta t_2) &= G_{1,2}(\theta_1, \theta_2) = G_1(\theta_2)G_1(\theta_1) = Q_2^{-1}S_2(\theta_2)Q_2Q_1^{-1}S_1(\theta_1)Q_1 \\
&= \begin{pmatrix} \cos(\theta_2) & i\frac{1}{\mu_2}\sin(\theta_2) \\ i\mu_2\sin(\theta_2) & \cos(\theta_2) \end{pmatrix} \begin{pmatrix} \cos(\theta_1) & i\frac{1}{\mu_1}\sin(\theta_1) \\ i\mu_1\sin(\theta_1) & \cos(\theta_1) \end{pmatrix} \\
&= \begin{pmatrix} \cos\theta_2\cos\theta_1 - \frac{\mu_1}{\mu_2}\sin\theta_1\sin\theta_2 & i\left[\frac{1}{\mu_1}\sin\theta_1\cos\theta_2 + \frac{1}{\mu_2}\cos\theta_1\sin\theta_2\right] \\ i[\mu_1\sin\theta_1\cos\theta_2 + \mu_2\cos\theta_1\sin\theta_2] & \cos\theta_2\cos\theta_1 - \frac{\mu_2}{\mu_1}\sin\theta_1\sin\theta_2 \end{pmatrix},
\end{aligned}
$$

where

$$\theta_i = \omega a_i \Delta t_i = \omega a_i m_i \varepsilon.$$

(The angular frequency of the disturbance in material i is $a_i\omega$, so θ_i is a measure of the disturbance frequency relative to the frequency of the laminate ε^{-1}.) In terms of the transmission coefficients, T and $\tilde{T}$, of a disturbance moving from one material to the next, as computed in the appendix, the amplification matrix is

$$
\begin{pmatrix} T_{1,2}\cos(\theta_1+\theta_2) + \tilde{T}_{1,2}\cos(\theta_1-\theta_2) & \frac{i}{\mu_1}[T_{1,2}\sin(\theta_1+\theta_2) + \tilde{T}_{1,2}\sin(\theta_1-\theta_2)] \\ i\mu_1[T_{2,1}\sin(\theta_1+\theta_2) + \tilde{T}_{2,1}\sin(\theta_1-\theta_2)] & T_{2,1}\cos(\theta_1+\theta_2) + \tilde{T}_{2,1}\cos(\theta_1-\theta_2) \end{pmatrix}.
$$

We can detect instability and stability by looking at the spectrum of this matrix. If ω is such that the spectrum of $G_{1,2}$ is greater than 1, then this mode is unstable as the energy in this mode increases and is stable otherwise. We note that Floquet analysis can also be used for this problem. The eigenvalues of $G_{1,2}$ are essentially equivalent to $e^{\nu\varepsilon}$ where ν is the Floquet exponent such that

$$\begin{pmatrix} \bar{z} \\ \bar{v} \end{pmatrix}(\omega, t) = e^{\nu\varepsilon}\begin{pmatrix} \bar{z} \\ \bar{v} \end{pmatrix}(\omega, t-\varepsilon).$$

Thus, $|e^{\nu\varepsilon}| > 1$ implies that the solution grows in time.

The determinant of $G_{1,2}$ is 1, and

$$
\begin{aligned}
\mathbf{T} \equiv \operatorname{trace}(G_{1,2}) &= 2\cos\theta_1\cos\theta_2 - R\sin\theta_1\sin\theta_2 \\
&= (1 + R/2)\cos(\theta_1+\theta_2) + (1 - R/2)\cos(\theta_1-\theta_2) \\
&= (1 + R/2)\cos(\theta_1(1+\alpha)) + (1 - R/2)\cos(\theta_1(1-\alpha)) = \mathbf{T}(\theta_1),
\end{aligned} \tag{6}
$$

where

$$\alpha = \theta_2/\theta_1 = a_2m_2/a_1m_1, \tag{7}$$

and

$$R = \frac{\mu_1}{\mu_2} + \frac{\mu_2}{\mu_1}. \tag{8}$$

Note that $R \geq 2$ with equality holding only when $\mu_1 = \mu_2$. The physics of the problem defines the fixed parameters R and α; θ_1 varies with the wave modes. The eigenvalues of $G_{1,2}$ are the roots of the characteristic equation $\sigma^2 - \mathbf{T}\sigma + 1$:

$$\sigma_{\pm} = \frac{\mathbf{T} \pm \sqrt{\mathbf{T}^2 - 4}}{2}.$$

If ω is such that $|\mathbf{T}| \leq 2$, $|\sigma_+| = |\sigma_-| = 1$, so this wave mode is stable. If ω is such that $|\mathbf{T}| > 2$, then $|\sigma_{\mathrm{sgn}(\mathbf{T})}| > \mathbf{T}/2 > 1$ and the ω mode is unstable.

When there is no contrast in impedance between material 1 and material 2 ($R = 2$), all modes are stable since the magnitude of $\mathbf{T}$ is bounded by 2.

Consider the case $R > 2$. From (6),

$$\frac{d\mathbf{T}}{d\theta_1} = -(1+\alpha)(1+R/2)\sin(\theta_1(1+\alpha)) - (1-\alpha)(1-R/2)\sin(\theta_1(1-\alpha)),$$
$$\frac{d^2\mathbf{T}}{d\theta_1^2} = -(1+\alpha)^2(1+R/2)\cos(\theta_1(1+\alpha)) - (1-\alpha)^2(1-R/2)\cos(\theta_1(1-\alpha)).$$

When $\omega = 0$, $\frac{d\mathbf{T}}{d\theta_1} = 0$ and $\frac{d^2\mathbf{T}}{d\theta_1^2}(0) < 0$, so $\mathbf{T}$ has a local maximum at $\theta_1 = 0$. Since $\mathbf{T}(0) = 2$, there exists $\delta > 0$, such that for $|\omega| \leq \delta$, $\mathbf{T} < 2$ and these modes are stable.

On the other hand, when $\theta_1 = \pi/(1+\alpha)$, and $R > 2$, the trace of matrix $G_{1,2}$ is $-(1 + R/2) + (1 - R/2)\cos(\pi(1-\alpha)/(1+\alpha))$, which can range between $-(1+R/2) + (1 - R/2) = -R < -2$ and $-(1+R/2) - (1-R/2) = -2$. The latter value is attained only if α is such that $(1-\alpha)/(1+\alpha) = n$ for n an odd integer. This would require $\alpha = (1 - n)/(1+n)$. This is impossible for $\alpha > 0$. Hence, we are guaranteed that for wave modes in a small enough neighborhood of $\omega = \pi/(1+\alpha)(a_1 m_1 \varepsilon)$ (i.e., with wavelengths that are $\mathcal{O}(a_1 m_1 \varepsilon)$) we have $|\mathbf{T}| > 2$ and hence amplitude growth.

From the preceding discussion, we may state the following: *There is inherent instability for the initial value problem of wave propagation through temporal laminates of contrasting impedance ($\mu_1 \neq \mu_2$). Long wave disturbances remain stable, while disturbances with wave lengths of the order of the material pattern are unstable.* Energy that is pumped into system at frequency $O(1/\varepsilon)$ to create the laminate is converted into energy of waves of comparable frequency and the amplitude of these oscillations grow.

Figure 1 below displays the spectrum of the amplification matrix $G_{1,2}$ as a function of the ratio of ν, the wavelength of the disturbance ($=\frac{2\pi}{\omega}$), to ε ($\sim$ the laminate "wavelength"), and as a function of θ_1, which indicates the ratio of the wave frequency in material 1 to that of the laminate. The two arguments are related according to $\nu/\varepsilon = 2\pi a_1 m_1/\theta_1$. For the laminate in this computation, the parameters are $(k_1, \rho_1) = (1, 1)$, $(k_1, \rho_2) = (10, 9)$, $m_1 = 0.5$, hence $\alpha = 1.054093$, $R = 9.592242$. It is illustrated in this figure that disturbances with wavelengths greater than $\mathcal{O}(\varepsilon)$ remain stable, while other shorter wave disturbances will become unstable.

3. NUMERICAL METHOD FOR LONG WAVE PROPAGATION

In homogenization, one is concerned with the $\varepsilon \to 0$ limit, so in the temporal laminate problem the wave impulse travels through more and more layers in finite time. In our work, we are interested in the behavior of disturbances whose wavelengths are long relative to

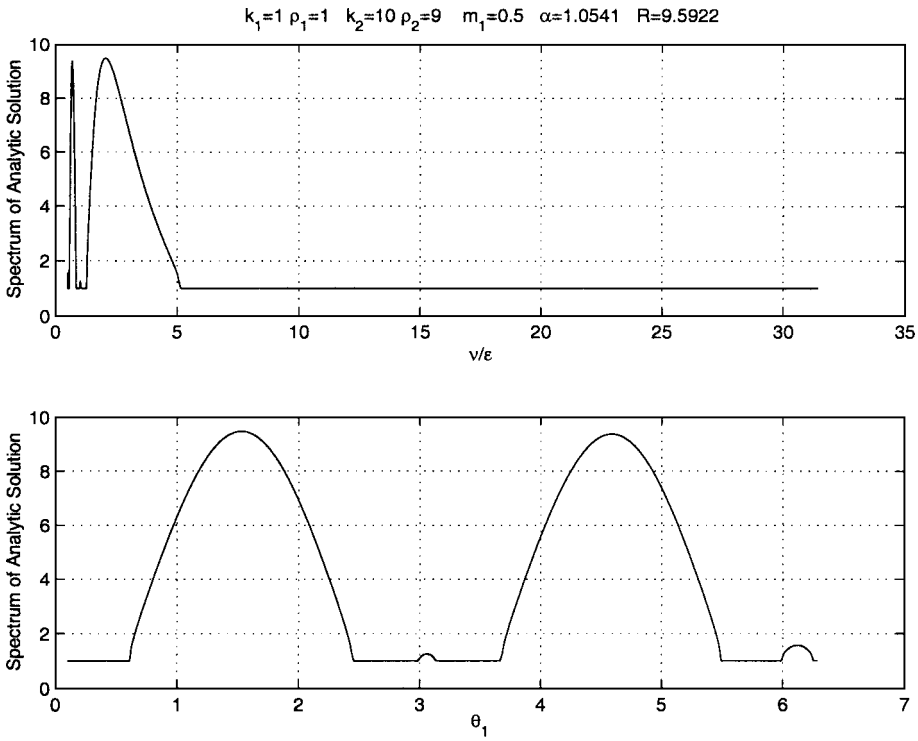

FIG. 1. Spectrum of the growth matrix for the analytic problem.

the period of the medium, i.e., $(1/\omega)/\varepsilon$ large or $\omega\varepsilon$ small, where ε is the wavenumber of the disturbance. From the analysis in Section 2, it is clear that for initial data made up of such modes, the problem is well posed. However, there will be difficulty in advancing the problem numerically even when the initial data is so restricted. This is because round-off, interpolation, and truncation errors introduce spurious disturbances into the computation. These perturbations will inevitably contain shorter wave modes which will be amplified by the due nature of the problem, and the computational results will be degraded.

We employ a standard first-order, upwind, finite-difference approximation to solve the system (3), (4) (or (5)). This numerical method adds numerical viscosity to the solution. We find that by appropriately controlling the size of the mesh width relative to the material property pattern, enough diffusion can be produced to damp modes so that they never grow during the numerical computation.

Consider a spatially uniform finite-difference grid with grid cells $[x_{j-1/2}, x_{j+1/2}]$. Let Δx denote the width of these cells and $x_j = (x_{j-1/2} + x_{j+1/2})/2$ denote the cell center. We take alternate time steps of size $\Delta t_1 = m_1\varepsilon$ and $\Delta t_2 = m_2\varepsilon$. Thus, material properties are constant within a space–time cell volume, and a single time step takes us from one material interface to the next. The nth time level is denoted by t_n and is the upper boundary of the nth individual material layer. The values of z and v at the grid points x_j at time t_n are denoted by z_j^n, v_j^n, and these values simultaneously represent the approximations to z and v at those points in space–time, as well as the values of z and v averaged over cell j at time t_n. We use $\rho_n, k_n, \mu_n, \ldots$ to denote the values of the respective material parameters between times t_n and t_{n+1} that is, in the $(n+1)$st material layer.

Integrating the conservation law (5) over the jth space–time cell volume from time t_n to time t_{n+1} gives

$$\left(z+\frac{v}{\mu_n}\right)_j^{n+1} = \left(z+\frac{v}{\mu_n}\right)_j^{n} + \frac{a_n}{\Delta x}\int_{t_n}^{t_{n+1}} \left[\left(z+\frac{v}{\mu_n}\right)\left(x_{j+1/2},t\right) - \left(z+\frac{v}{\mu_n}\right)\left(x_{j-1/2},t\right)\right] dt \tag{9}$$

$$\left(z-\frac{v}{\mu_n}\right)_j^{n+1} = \left(z-\frac{v}{\mu_n}\right)_j^{n} - \frac{a_n}{\Delta x}\int_{t_n}^{t_{n+1}} \left[\left(z-\frac{v}{\mu_n}\right)\left(x_{j+1/2},t\right) - \left(z-\frac{v}{\mu_n}\right)\left(x_{j-1/2},t\right)\right] dt. \tag{10}$$

Conservative techniques distinguish themselves from each other by their approximations to the fluxes $\int z,\, v(x_{j+1/2},t)$. Since our equations (5) are linear, we calculate the values of $z+v/\mu$, $z-v/\mu$ along the cell interfaces in a straightforward manner by tracing characteristics. Thus,

$$\int_{t_n}^{t_{n+1}} (z+v/\mu_n)\left(x_{j+1/2},t\right) = \frac{1}{a_n}\int_{x_{j+1/2}}^{x_{j+1/2}+a_j\Delta t} (z+v/\mu_n)(x,t_n)\,dx,$$

$$\int_{t_n}^{t_{n+1}} (z-v/\mu_n)\left(x_{j+1/2}(t),t\right) = \frac{1}{a_n}\int_{x_{j+1/2}-a_j\Delta t}^{x_{j+1/2}} (z-v/\mu_n)(x,t_n)\,dx,$$

where $\Delta t_n = t_{n+1}-t_n$. Since z_j^n, v_j^n are cell-averaged, cell-centered values of z and v in the jth cell, the first-order reconstruction of the profiles are piecewise constant taking on the values $\cdot_j^n$ in cell j. Equations (9) and (10) are approximated by

$$z_j^{n+1}+\frac{v_j^{n+1}}{\mu_n} = z_j^n+\frac{v_j^n}{\mu_n}+\frac{a_n\Delta t_n}{\Delta x}\left[\left(z_{j+1}^n+\frac{v_{j+1}^n}{\mu_n}\right)-\left(z_j^n+\frac{v_j^n}{\mu_n}\right)\right]$$

$$z_j^{n+1}-\frac{v_j^{n+1}}{\mu_n} = z_j^n-\frac{v_j^n}{\mu_n}-\frac{a_n\Delta t_n}{\Delta x}\left[\left(z_j^n-\frac{v_j^n}{\mu_n}\right)-\left(z_{j-1}^n-\frac{v_{j-1}^n}{\mu_n}\right)\right],$$

and by combining the equations above, the system (3), (4) is approximated by the solutions to the finite-difference method,

$$z_j^{n+1} = z_j^n+\frac{1}{\rho_n}\frac{\Delta t_n}{2\Delta x}\left[v_{j+1}^n-v_{j-1}^n\right]+\frac{a_n\Delta t_n}{2\Delta x}\left(z_{j+1}^n-2z_j^n+z_{j-1}^n\right), \tag{11}$$

$$v_j^{n+1} = v_j^n+k_n\frac{\Delta t_n}{2\Delta x}\left[z_{j+1}^n-z_{j-1}^n\right]-\frac{a_n\Delta t_n}{2\Delta x}\left(v_{j+1}^n-2v_j^n+v_{j-1}^n\right), \tag{12}$$

and is accurate up to $\mathcal{O}(\Delta t,\Delta x)$.

For a, k, and ρ constant in time, this scheme is stable under the CFL restriction $a\Delta t_n/\Delta x\le 1$. We note also that the scheme has built in numerical viscosity since it approximates the PDE system

$$z_t-\frac{1}{\rho}v_x = (1-\lambda)\frac{a\Delta x}{2}z_{xx}, \tag{13}$$

$$v_t-kz_x = (1-\lambda)\frac{a\Delta x}{2}v_{xx}, \tag{14}$$

up to $\mathcal{O}(\Delta t^2,\Delta x^2)$ when $\lambda=\frac{a\Delta t}{\Delta x}$ is less than unity.

THEOREM 3.1. *Let* $\alpha = a_2 m_2 / a_1 m_1$, *and* $R = \mu_2/\mu_1 + \mu_1/\mu_2$. *Then the scheme* (11), (12) *above is stable for the temporal laminate problem when* Δx *is such that*

$$a_1 m_1 \frac{\varepsilon}{\Delta x} \leq \min\{1, 1/\alpha, \bar{\lambda}\}. \tag{15}$$

The relevant quantities are defined as

$$\bar{\lambda} = \begin{cases} 1 & \text{if } R = 2, \\ \lambda_\star & \text{if } \lambda_\star \leq \lambda_0,\ R \neq 2, \\ \lambda_{\star\star}, & \text{if } \lambda_\star > \lambda_0,\ R \neq 2, \end{cases}$$

and

$$\lambda_0 = \frac{2(1+\alpha)}{\alpha(R+6)}, \quad \lambda_\star = \frac{1+\alpha}{4\alpha} - \frac{|1-\alpha|}{4\alpha}\sqrt{\frac{R-2}{R+2}}, \quad \lambda_{\star\star} = 2\frac{\sqrt{\alpha^2 + R\alpha + 1} - (\alpha+1)}{\alpha(R-2)}.$$

Proof. To study the stability of the scheme, we perform a von Neumann analysis and look at the effect of the scheme on individual Fourier modes with wavenumber ω,

$$\begin{pmatrix} z \\ v \end{pmatrix}(x, t_n) = \begin{pmatrix} \bar{z} \\ \bar{v} \end{pmatrix} e^{i\omega x}.$$

By expressing the scheme as

$$\begin{aligned} \begin{pmatrix} z \\ v \end{pmatrix}_j^{n+1} &= \begin{pmatrix} 1-\lambda_n & 0 \\ 0 & 1-\lambda_n \end{pmatrix} \begin{pmatrix} z \\ v \end{pmatrix}_j^n \\ &\quad + \begin{pmatrix} \lambda_n/2 & -\lambda_n/2\mu_n \\ -\lambda_n\mu_n/2 & \lambda_n/2 \end{pmatrix} \begin{pmatrix} z \\ v \end{pmatrix}_{j-1}^n + \begin{pmatrix} \lambda_n/2 & \lambda_n/2\mu_n \\ \lambda_n\mu_n/2 & \lambda_n/2 \end{pmatrix} \begin{pmatrix} z \\ v \end{pmatrix}_{j+1}^n, \end{aligned}$$

it is easy to see that

$$\begin{pmatrix} \bar{z} \\ \bar{v} \end{pmatrix}_j^{n+1} = G_n(\theta) \begin{pmatrix} \bar{z} \\ \bar{v} \end{pmatrix}_j^n,$$

where

$$G_n = \begin{pmatrix} p_n & i b_n \\ i c_n & p_n \end{pmatrix}.$$

The entries of the matrix are

$$\begin{aligned} &\lambda_n = a_n \Delta t_n / \Delta x, \quad p_n = 1 - \lambda_n + \lambda_n \cos(\theta), \\ &b_n = \lambda_n \sin(\theta)/\mu_n, \quad c_n = \lambda_n \mu_n \sin(\theta), \end{aligned}$$

where $\theta = \omega \Delta x$. The eigenvalues of G_n are $(1-\lambda_n) + \lambda_n e^{\pm i\theta}$. The spectrum of G_n is therefore bounded by 1 in absolute value for all θ when $\lambda_n \leq 1$, and $\det(G_n) = 1 - 2\lambda_n(1-\lambda_n)(1-\cos(\theta))$ lies between 0 and 1. Wave modes do not grow in amplitude through a pure material.

However, as a disturbance goes from time t_n to time t_{n+2} under our scheme through a layer of material 1 followed by a layer of material 2, say, the modes grow or decay according to

$$\begin{pmatrix}\bar{z}\\ \bar{v}\end{pmatrix}_j^{n+2} = G_2(\theta)G_1(\theta)\begin{pmatrix}\bar{z}\\ \bar{v}\end{pmatrix}_j^{n},$$

where the amplification matrix is

$$G(\theta) = G_2(\theta)G_1(\theta) = \begin{pmatrix} p_2 & ib_2 \\ ic_2 & p_2 \end{pmatrix}\begin{pmatrix} p_1 & ib_1 \\ ic_1 & p_1 \end{pmatrix}. \tag{16}$$

The eigenvalues $\sigma_\pm$ of $G(\theta)$ solve the characteristic equation $\sigma^2 - B\sigma + C = 0$, where $B = \text{trace}(G)$ and $C = \det(G)$ are both real numbers. Now $|C| = |\det(G_1)||\det(G_2)| \le 1$, for $0 \le \lambda_1, \lambda_2 \le 1$, so if $B^2 - 4C \le 0$, then $\sigma_\pm = 0.5(B \pm i\sqrt{4C - B^2})$, and $|\sigma_\pm|^2 = |C|^2 \le 1$ for all θ. Thus, we can ensure that the spectrum of G is less than or equal to 1 if λ_1, λ_2 are such that $B^2 - 4C \le 0$ for all θ.

For stability, it thus suffices to find $\lambda_1, \lambda_2 \le 1$ such that $B^2 - 4C \le 0$ for all θ. From Eq. (16),

$$\begin{aligned}\text{trace}(G) &= B = 2p_2p_1 - (b_2c_1 + b_1c_2),\\ \det(G) &= C = \left(p_2^2 + b_2c_2\right)\left(p_1^2 + b_1c_1\right).\end{aligned}$$

Let $\lambda \equiv \lambda_1$ and $\alpha\lambda = \lambda_2$ whence $\alpha = a_2m_2/a_1m_1$. Then the first stability restriction is that

$$\lambda \le \min\{1, 1/\alpha\}. \tag{17}$$

The condition $B^2 - 4C \le 0$ is equivalent to

$$\begin{aligned}&(2p_2p_1 - (b_2c_1 + b_1c_2))^2 - 4\left(p_2^2 + b_2c_2\right)\left(p_1^2 + b_1c_1\right) \le 0\\ &\quad\Leftrightarrow (b_2c_1 - b_1c_2)^2 - 4(p_1c_2 + p_2c_1)(p_1b_2 + p_2b_1) \le 0\\ &\quad\Leftrightarrow \lambda^4\alpha^2(R^2 - 4)\sin^4\theta - 4\lambda^2\sin^2\theta[1 + R\alpha + \alpha^2 - \lambda\alpha(1 - \cos\theta)(\alpha + 1)(R + 2)]\\ &\qquad - 4\lambda^2\sin^2\theta[\alpha^2\lambda^2(1 - \cos\theta)^2(R + 2)] \le 0\\ &\quad\Leftrightarrow \lambda^2\alpha^2(R^2 - 4)\sin^2\theta - 4[1 + R\alpha + \alpha^2 - \lambda\alpha(1 - \cos\theta)(\alpha + 1)(R + 2)]\\ &\qquad - 4[\alpha^2\lambda^2(1 - \cos\theta)^2(R + 2)] \le 0\\ &\quad\Leftrightarrow \lambda^2\alpha^2(R + 2)[(R - 2)\sin^2\theta - 4(1 - \cos\theta)^2]\\ &\qquad + 4\alpha\lambda(R + 2)(1 - \cos\theta)(1 + \alpha) - 4[1 + R\alpha + \alpha^2] \le 0,\end{aligned}$$

where $R = \mu_1/\mu_2 + \mu_2/\mu_1 \ge 2$. Define the function $f(\lambda, \theta)$ as follows:

$$\begin{aligned}f(\lambda, \theta) = {}& \lambda^2\alpha^2(R + 2)[(R - 2)\sin^2\theta - 4(1 - \cos\theta)^2]\\ &+ 4\alpha\lambda(R + 2)(1 - \cos\theta)(1 + \alpha) - 4[1 + R\alpha + \alpha^2].\end{aligned} \tag{18}$$

We must find $\lambda > 0$ such that $f(\lambda, \theta) \le 0$ for $\theta \in [0, \pi]$.

When $R = 2$, that is, no impedance contrast, we have

$$\begin{aligned} f(\lambda, \theta) &= -16[\alpha\lambda(1 - \cos\theta)]^2 + 16(1 + \alpha)[\alpha\lambda(1 - \cos\theta)] - 4(1 + \alpha)^2 \\ &= -4[\alpha\lambda(1 - \cos\theta) - 2(1 + \alpha)]^2 \leq 0. \end{aligned}$$

The only stability restriction in this case is (17), thus it suffices to say $\bar{\lambda} = 1$ as in the statement of the theorem.

Henceforth, assume $R > 2$. For any given λ, f has extrema at θ solving

$$\frac{\partial f}{\partial \theta} = 2\alpha\lambda(R + 2)\sin\theta[2(1 + \alpha) + \alpha\lambda((R + 2)\cos\theta - 4)] = 0.$$

Thus, when $\theta = 0, \pi$ or when

$$\cos\tilde{\theta} = \frac{4\alpha\lambda - 2\alpha - 2}{(R + 2)\alpha\lambda}, \tag{19}$$

f attains its local extrema. The right-hand side of the expression above is always less than or equal to 1, so $\tilde{\theta}$ exists when $\cos(\tilde{\theta}) = \frac{4\alpha\lambda - 2\alpha - 2}{(R+2)\alpha\lambda} \geq -1$. That is, when $\lambda \geq \lambda_0$, for

$$\lambda_0 = \frac{2(1 + \alpha)}{\alpha(R + 6)}. \tag{20}$$

One may check that $\frac{\partial^2 f}{\partial \theta^2}(\lambda, 0) > 0$, so there is a local minimum at $\theta = 0$; thus when $\lambda \geq \lambda_0$, $\tilde{\theta}$ is the local and absolute maximum on $[0, \pi]$.

From (18), $f(\lambda, 0) = -4(1 + R\alpha + \alpha^2)$ and

$$f(\lambda, \pi) = f(\lambda, 0) + 8\alpha\lambda(1 + \alpha - 2\alpha\lambda),$$

so $f(\lambda, \pi) \geq f(\lambda, 0)$ iff $\lambda \leq \frac{1+\alpha}{2\alpha}$. Since $\lambda_0 < \frac{1+\alpha}{2\alpha}$, we may conclude that

- for $\lambda \leq \lambda_0$, the maximum value of f is $f(\lambda, \pi)$;
- for $\lambda > \lambda_0$, the maximum value of f is $f(\lambda, \tilde{\theta})$,

$$(R - 2)[(\alpha\lambda)^2(R - 2) + 4(\alpha + 1)(\alpha\lambda) - 4\alpha], \tag{21}$$

using (19) and (18).

We must check for what λ these maximum values are nonpositive for all $\theta \in [0, \pi]$.

First, $f(\lambda, \pi) \leq 0$ for

$$\lambda \leq \lambda_\star = \frac{1 + \alpha}{4\alpha} - \frac{|1 - \alpha|}{4\alpha}\sqrt{\frac{R - 2}{R + 2}}, \quad \lambda \geq \frac{1 + \alpha}{4\alpha} + \frac{|1 - \alpha|}{4\alpha}\sqrt{\frac{R - 2}{R + 2}}.$$

When $R > 2$, $(1 + \alpha)/4\alpha > \lambda_0$, so we focus on the first inequality above and conclude that if $\lambda_\star < \lambda_0$, it is guaranteed that $f(\lambda, \theta)$ is non-positive for $0 < \lambda \leq \lambda_\star$, but will be positive for $\lambda_\star < \lambda < \lambda_0$. On the other hand, if $\lambda_\star \geq \lambda_0$, it is guaranteed that $f(\lambda, \theta)$ is non-positive for $0 < \lambda \leq \lambda_0$, and possibly beyond.

Next, from (21), $f(\lambda, \tilde{\theta}) \leq 0$ when $\lambda \leq \lambda_{\star\star}$, for

$$\lambda_{\star\star} = \frac{-2(1 + \alpha) + 2(\sqrt{\alpha^2 + R\alpha + 1})}{\alpha(R - 2)}. \tag{22}$$

If $\lambda_\star > \lambda_0$, then $0 > f(\lambda_0, \pi) = f(\lambda_0, \tilde{\theta})$. Thus, $\lambda_0 < \lambda_{\star\star}$, and we may then say $f(\lambda, \theta)$ is non-positive for $0 < \lambda \leq \lambda_{\star\star}$.

Thus, the second stability restriction for is that

$$\lambda \leq \bar{\lambda},$$

where

$$\bar{\lambda} = \begin{cases} \lambda_\star & \text{if } \lambda_0 > \lambda_\star \\ \lambda_{\star\star} & \text{otherwise.} \end{cases}$$

This, together with the defintion $\bar{\lambda} = 1$ when $R = 2$ and (17), proves the theorem.

Besides the addition of numerical viscosity to the system of equations, one can consider another mechanism acting to give stability of the new scheme. As we mentioned in Section 2, disturbances with wavelengths greater than $\mathcal{O}(\varepsilon)$ will remain stable, while shorter wave disturbances may become unstable. Since the shortest wavelength that can be resolved on the grid is $2\Delta x$, by choosing Δx large enough to obey the CFL restriction in (15), we are bounding from below the ratio of the computationally realizable wavelengths to the laminate frequency ε, thus pushing us further into the stable zone.

Figures 2 and 3 display the spectrum of the numerical amplification matrix G as a function of the ratio of ν, the wavelength of the disturbance, to ε, and as a function of θ. The two arguments are related according to $\frac{\nu}{\varepsilon} = 2\pi a_1 m_1 / \lambda_1 \theta$. For this laminate, the parameters are $(k_1, \rho_1) = (1, 1)$, $(k_2, \rho_2) = (10, 9)$, $m_1 = 0.5$, hence $\alpha = 1.054093$, $R = 9.592242$.

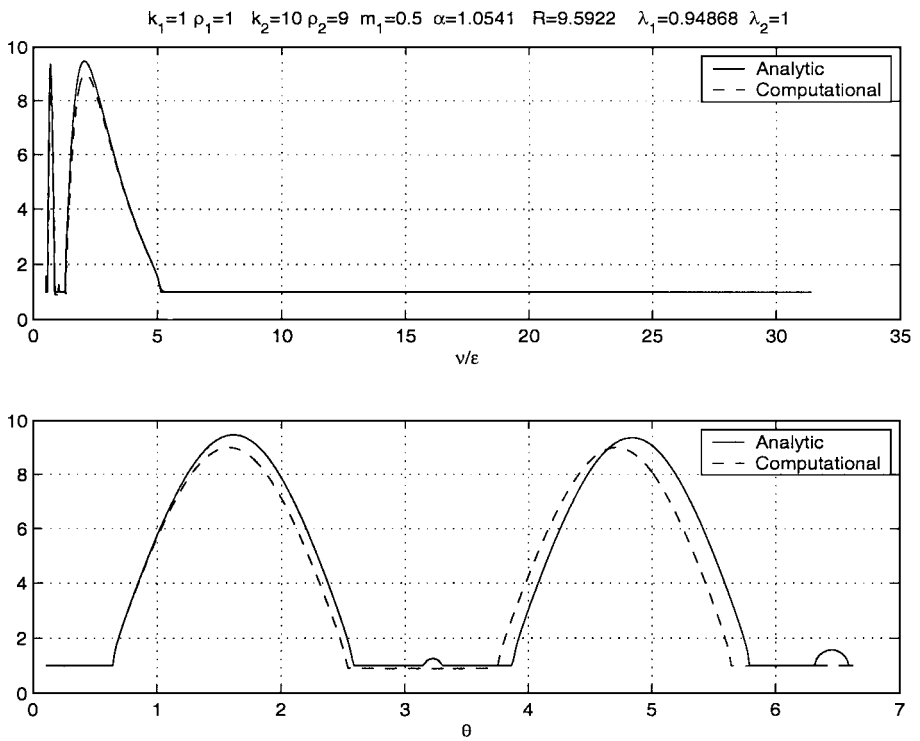

FIG. 2. Spectrum of the growth matrix under the traditional constraint $\max(\lambda_1, \lambda_2) = 1$.

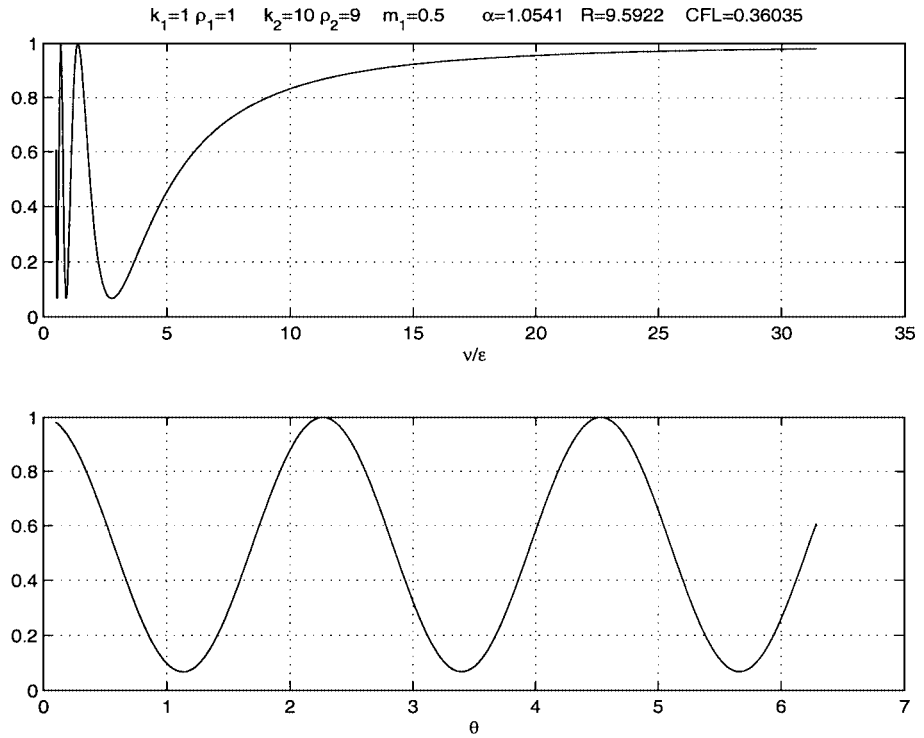

FIG. 3. Spectrum of the growth matrix under the newly derived stability restriction in (15).

Figure 2 shows that under the traditional CFL conditions where we take max $(\lambda_1, \lambda_2) = 1$, shorter wavelengths are amplified. Figure 3 shows that under the new CFL constraints in (15), where $\bar{\lambda} = 0.360352$ for this example, the scheme remains stable for all wavelengths.

4. NUMERICAL RESULTS AND DISCUSSION

We conclude this article by presenting the results of some numerical computations which illustrate the stability/instability effects of computing the temporal laminate problem. Consider the temporal laminate problem $(\rho z_t)_t - k z_{xx}$, with parameters

$$(k_1, \rho_1) = (1, 1), \quad (k_2, \rho_2) = (10, 9), \quad m_1 = 0.5, \tag{23}$$

and initial data

$$z(x, 0) = e^{-x^2}, \quad z_t(x, 0) = 0. \tag{24}$$

The period of the laminate is 0.01. These smooth initial data have a support of width greater than 4. Figures 4 and 5 below show the numerically averaged solution $\langle z \rangle$. This computation is performed with the scheme given in the previous section using the upper limit of the stability constraint in (15). In this case $\bar{\lambda} = 0.360352$, which determines the grid size for the computation. We use a trapezoidal rule to approximate $\langle z \rangle_j$, which is $z(x_j, \cdot)$ averaged over a period of the laminate. Thus, for the qth period, which goes from $t = t_{2q}$

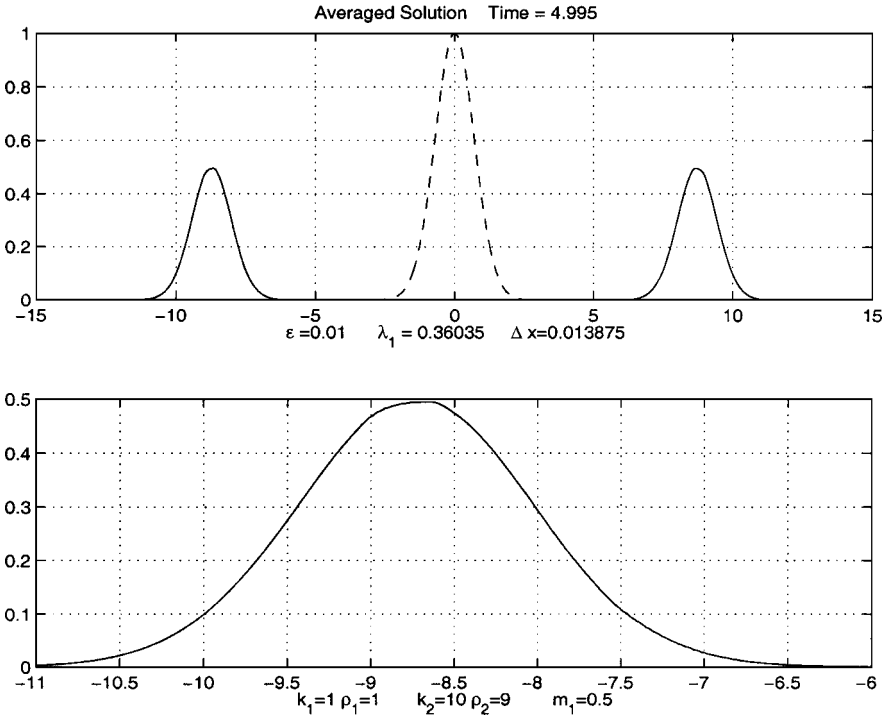

FIG. 4. Averaged solution to the temporal laminate problem with initial data (24), parameters (23), and stability constraint (15).

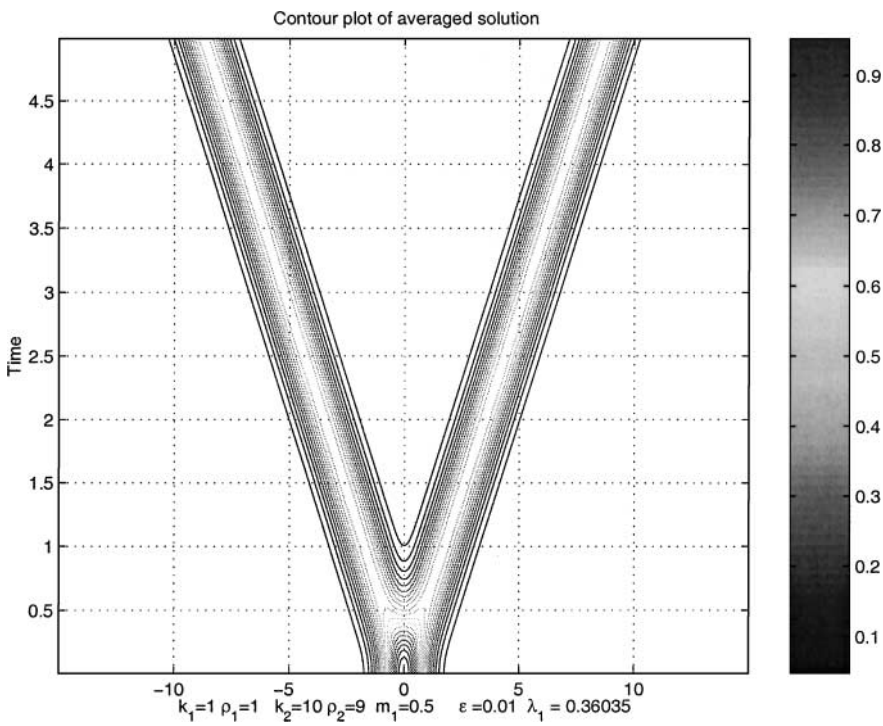

FIG. 5. Contour plot up to time 4.995 of the evolution of the averaged solution to the temporal laminate problem with initial data (24), parameters (23), and stability constraint (15).

to t_{2q+2},

$$\langle z\rangle_j = \frac{1}{2}\left(m_1 z_j^{2q} + z_j^{2q+1} + m_2 z_j^{2q+2}\right).$$

Recall that $t_{2q+1} - t_{2q} = m_1\varepsilon$ and $t_{2q+2} - t_{2q+1} = m_2\varepsilon$ with $m_1 + m_2 = 1$. The averaged solution is shown after traveling through 500 laminate layers. The 500th laminate spans the time interval [4.99, 5], so the solution is represented as time 4.995. We see very stable behavior. In the lower plot of Fig. 4, we have zoomed in on the left-going D'Alembert wave. For the data used, the theoretical homogenization speed (2) is 1.748015, so at time 4.995 the average disturbance should travel a distance 8.7313 from the origin. The numerical results and the theory agree quite well.

Figure 6 shows the same problem computed up to time 0.075 with the constraint that $\max(\lambda_1, \lambda_2) = 1$. The instability due to the growth of the smaller wave modes is apparent even through just seven laminate layers. Computing beyond this time is pointless, as the unstable modes destroy the solution.

Note that in the example used, the effective wave speed 1.748015 is greater than the speeds in the individual materials, which are 1 and 1.0541. The homogenization speed predicted by the theory is $\sqrt{\langle 1/\rho\rangle\langle k\rangle}$. Thus, it is easy to show that the effective speed is greater than the individual phase speeds if and only if

$$-2\Delta\rho\Delta k < \rho_1\Delta k - k_2\Delta\rho < 0, \tag{25}$$

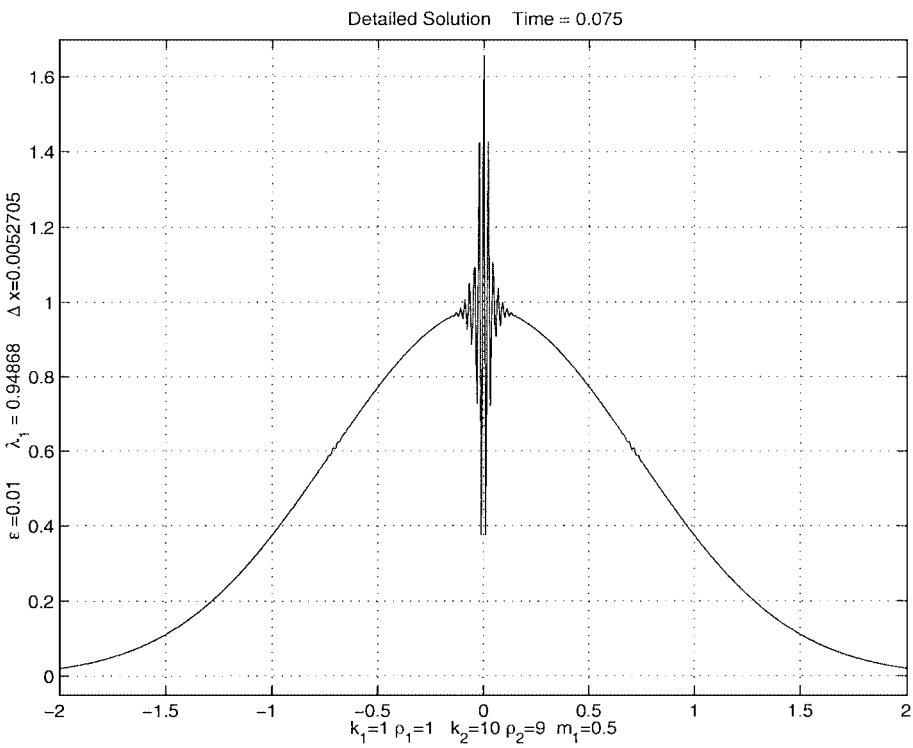

FIG. 6. Instability at time 0.075 in the solution of the temporal laminate problem with initial data (24), parameters (23), and Δx such that $\min(\lambda_1, \lambda_2) = 1$.

where $\Delta\rho = \rho_2 - \rho_1$ and $\Delta k = k_2 - k_1$. Thus, in an electromagnetic application, by varying the permeability and permittivity temporally, we can make electromagnetic signals travel faster than they would in either pure medium. The parameters that we used in the computational examples in Figs. 4 and 5 satisfy the conditions in (25) since $\Delta\rho = 8$, $\Delta k = 9$ and $\rho_1 = 1$, $k_2 = 10$.

The numerical approach developed here is useful for problems where homogenization techniques are difficult to apply, e.g., for problems on finite domains and for the checkerboard spatio-temporal configuration in the (x, t) plane. Moreover, by the change of variables $\tau = t - x/V$ and $\zeta = x$, the fast-range (supersonic) laminate problem with $|V| > a_i$ becomes a temporal laminate problem in the (ζ, τ) plane,

$$\rho z_\tau + \frac{1}{V} v_\tau = v_\zeta,$$
$$\frac{1}{k} v_\tau + \frac{1}{V} z_\tau = z_\zeta.$$

The methods used to study the temporal laminate problem can then be applied to the investigation of the instability properties of the supersonic problem. The development of an appropriate numerical method will be the subject of another article.

In this work, it has been made clear that energy plays an important and interesting role in wave propagation through temporal and supersonic laminates. Prompted by this finding, we consider further novel energy issues in [11].

APPENDIX

Reflection and Transmission Coefficients

Consider wave motion, governed by $(\rho z_t)_t - k z_{xx} = 0$, through a material, homogeneous in space, with material values given by

$$(k, \rho) = \begin{cases} (k_1, \rho_1) & \text{for } t < 0, \\ (k_2, \rho_2) & \text{for } t < 0. \end{cases}$$

We investigate the waves that result when an incident wave traveling through material 1, experiences the switch in material values at time $t = 0$, and now is moving in material 2. Without loss of generality, the analysis is carried out for the case of a disturbance $s(x + a_1 t)$ moving at velocity $-a_1$.

At the interface $t = 0$, we require continuity of the disturbance and its momentum:

$$\lim_{t \to 0^-} z(x, t) = \lim_{t \to 0^+} z(x, t), \tag{26}$$

$$\lim_{t \to 0^-} \rho_1 \frac{\partial z}{\partial t}(x, t) = \lim_{t \to 0^+} \rho_2 \frac{\partial z}{\partial t}(x, t). \tag{27}$$

In general, a disturbance will take the form

$$z(x, t) = f_1(x - a_1 t) + g_1(x + a_1 t), \quad t < 0, \tag{28}$$

$$z(x, t) = f_2(x - a_2 t) + g_2(x + a_2 t), \quad t > 0, \tag{29}$$

where $a_i = \sqrt{k_i/\rho_i}$ is the speed of sound through material i. From our assumption on the nature of the disturbance in material 1, it is clear that $f_1 = 0$ and $g_1(x) = s(x)$. The interface compatibility conditions, (26), (27), are then

$$\begin{aligned} s(x) &= f_2(x) + g_2(x), \\ \rho_1 a_1 s'(x) &= \rho_2 a_2 (g_2'(x) - f_2'(x)). \end{aligned} \tag{30}$$

Integrating this latter equation with respect to x gives

$$\mu_1 s(x) = \mu_2 (g_2(x) - f_2(x)), \tag{31}$$

where $\mu_1 = \rho_i a_i$ is called the material impedance. By solving (30) and (31) together, we get that

$$f_2(x) = T_{1,2} s(x), \quad g_2(x) = \tilde{T}_{1,2} s(x),$$

where

$$T_{1,2} = \frac{\mu_2 + \mu_1}{2\mu_2}, \quad \tilde{T}_{1,2} = \frac{\mu_2 - \mu_1}{2\mu_2}.$$

So, by (28) and (29), the solution is

$$\begin{aligned} z(x,t) &= T_{1,2}\, s(x + a_2 t) + \tilde{T}_{1,2}\, s(x - a_2 t), \quad t > 0, \\ z(x,t) &= s(x + a_1 t), \quad t < 0. \end{aligned}$$

That is, on experiencing the material switch, the incident wave s breaks into waves with amplitudes magnified by the amounts $\tilde{T}_{1,2}$ and $\tilde{T}_{1,2}$ (transmission coefficients). Similarly, for an initial disturbance $s(x - a_1 t)$, moving through the material with parameters (ρ_1, k_1), and experiencing a switch to parameters (ρ_2, k_2) at time $t = 0$, the solution is

$$z(x,t) = T_{1,2}\, s(x - a_2 t) + \tilde{T}_{1,2}\, s(x + a_2 t), \quad t > 0, \tag{32}$$

$$z(x,t) = s(x - a_2 t), \quad t < 0. \tag{33}$$

For a disturbance in the dual variable v, replace $T(\tilde{T})_{1,2}$ by $T(\tilde{T})_{2,1}$. For example, $v(x,t) = T_{2,1}\, s(x - a_2 t) + \tilde{T}_{2,1}\, s(x + a_2 t)$ for $t > 0$ when $v(x,t) = s(x - a_2 t)$ for $t < 0$.

Note that by looking at the coefficient of x, it is clear that a wave of a given wavenumber gives birth to new waves of the same wavenumber. That is, no new wavenumbers should be observed.

REFERENCES

1. K. A. Lurie, Effective properties of smart elastic laminates and the screening phenomenon, *Int. J. Solids Structures* **34**, 1633 (1997).
2. K. A. Lurie, Control in the coefficients of linear hyperbolic equations via spatio-temporal composites, in *Homogenization*, edited by V. Berdichevsky, V. Jikov, and G. Papanicolaou, Series on Advances in Mathematics for Applied Sciences (World Scientific, Singapore, 1999), Vol. 50.
3. S. L. Weekes, Numerical modelling of wave phenomena in dynamic materials, *Appl. Numer. Math.* **37**, 417 (2001).

4. A. Bensoussan, J. L. Lions, and G. Papanicolaou, *Asymptotic Analysis for Periodic Structures* (North-Holland, Amsterdam, 1978).
5. E. H. Lee and W. H. Yang, On waves in composite materials with periodic structures, *SIAM J. Appl. Math.* **25**, 492 (1973).
6. E. Sanchez-Palencia, *Nonhomogeneous Media and Vibration Theory*, Lecture Notes in Physics (Springer-Verlag, Berlin, 1980), Vol. 127.
7. F. Santosa and W. W. Symes, A dispersive effective medium for wave propagation in periodic composites, *SIAM J. Appl. Math.* **51**, 984 (1991).
8. L. Brillouin, *Wave Propagation in Periodic Structures* (Dover, New York, 1953).
9. J. J. Stoker, *Nonlinear Vibrations in Mechanical and Electrical Systems* (Interscience, New York, 1950).
10. T. R. Fogarty and R. J. LeVeque, High resolution finite volume methods for acoustic waves in periodic and random media, *J. Acoust. Soc. Amer.* **106**, 17 (1999).
11. K. A. Lurie and S. L. Weekes, spatio-temporal dielectric composites with negative values of ϵ and μ and negative energy density, submitted for publication.